THE JOURNAL OF BIOLOGICAL CHEMISTRY VOL. 287, NO. 48, pp. 40246–40255, NOvember 23, 2012

Irregular Ca^{2+} Oscillations Regulate Transcription via Cumulative Spike Duration and Spike Amplitude*[S]

Received for publication, September 7, 2012, and in revised form, October 14, 2012 Published, JBC Papers in Press, October 15, 2012, DOI 10.1074/jbc.M112.417154

Shanshan Song[‡§1], **Jiansha Li**[§¶1], **Liping Zhu**[‡§], **Lei Cai**[‡§], **Qian Xu**[‡§], **Chen Ling**[‡§], **Yuan Su**[§‖], **and Qinghua Hu**[‡§**2]

From the [‡]*Department of Pathophysiology,* [§]*Key Laboratory of Pulmonary Diseases of Ministry of Health of China,* [¶]*Department of Pathology,* [‖]*Department of Respiratory Medicine, Union Hospital, and the* **MOE Key Laboratory of Environment and Health, *School of Public Health, Tongji Medical College, Huazhong Science and Technology University, Wuhan 430030, People's Republic of China*

Background: $[Ca^{2+}]_i$ oscillations are irregular and heterogeneous.
Results: The correlations between NFκB/STAT3-GFP transcription and $[Ca^{2+}]_i$ spike amplitude/cumulative spike duration are revealed by simultaneous monitoring in single cells and validated in cell population.
Conclusion: $[Ca^{2+}]_i$ oscillations regulate transcription through $[Ca^{2+}]_i$ spike amplitude and cumulative spike duration.
Significance: How irregular $[Ca^{2+}]_i$ oscillations control transcription is crucial for understanding biological $[Ca^{2+}]_i$ signal-regulated events.

Agonist-stimulated $[Ca^{2+}]_i$ oscillations are universally irregular in their kinetics. How irregular $[Ca^{2+}]_i$ oscillations dynamically regulate agonist-stimulated downstream events has not been studied. To overcome the obstacles of irregularity and heterogeneity of $[Ca^{2+}]_i$ oscillations, agonist-stimulated $[Ca^{2+}]_i$ signaling and NFκB/STAT3-GFP nuclear translocation were simultaneously monitored in each single cell examined. The cause-effect relationship between $[Ca^{2+}]_i$ oscillation parameters and transcriptional activities was validated in cell populations through irregular $[Ca^{2+}]_i$ oscillations with varied parameters. The time duration of cumulative $[Ca^{2+}]_i$ elevations reaching the threshold $[Ca^{2+}]_i$ level for a transcriptional factor activation and $[Ca^{2+}]_i$ spike amplitude was found to control agonist-stimulated transcription and gene expression.

$[Ca^{2+}]_i$ oscillations have been observed in all types of cells ever studied (1, 2), and the (patho-)biological way to evoke $[Ca^{2+}]_i$ oscillations is via the stimulation of a cell membrane receptor by its agonist (3). The kinetics of this universal phenomenon are irregular (4–15). The irregularity means that the kinetic parameters like $[Ca^{2+}]_i$ spike amplitude vary by time after agonist stimulation in one cell. Additionally, the kinetic parameters are heterogeneous between cells examined even at the same time. Irregularity and heterogeneity of $[Ca^{2+}]_i$ oscillations prevented us from revealing experimentally how $[Ca^{2+}]_i$ oscillations really encode their downstream events like transcription.

In previous investigations in regular $[Ca^{2+}]_i$ oscillations, it has been established that $[Ca^{2+}]_i$ oscillations regulate downstream events through their kinetic parameters, *e.g.* $[Ca^{2+}]_i$ spike amplitude and frequency (17–20), and the frequency-dependent regulation is probably through cumulative spike duration (CSD) of $[Ca^{2+}]_i$ level arriving at the threshold for the activation of a downstream event (20). All of the above understandings are based on experimental studies employing $[Ca^{2+}]_i$ oscillations models with manipulated parameters revealing the cause-effect relationship between each parameter and a downstream event. In those studies (17–20), however, $[Ca^{2+}]_i$ oscillations were generated and maintained with constant or regular parameters such as $[Ca^{2+}]_i$ interspike interval, spike duration, and spike amplitude for each of the conditions employed during experimental period in each individual cell and among different cells. Therefore, those $[Ca^{2+}]_i$ oscillation models are actually only representing regular $[Ca^{2+}]_i$ oscillations. Furthermore, $[Ca^{2+}]_i$ oscillations models by themselves are not directly biologically relevant. How agonist-stimulated, biologically relevant $[Ca^{2+}]_i$ oscillations featured by kinetic irregularity and heterogeneity dynamically regulate its downstream events remains unknown.

To undertake this challenge, experiments need to be conducted to conquer the obstacles of kinetic irregularity and heterogeneity in $[Ca^{2+}]_i$ oscillations. Therefore, simultaneously monitoring a $[Ca^{2+}]_i$ signal and a $[Ca^{2+}]_i$-dependent transcriptional activation in each individual cell was performed in the current study to reveal the quantitative correlation between parameters and downstream events. To validate the correlative relationship, the recently established $[Ca^{2+}]_i$ oscillations model in cell populations (19, 20) mimicking the predominant pattern of the irregular calcium oscillations was employed. Our study shows that agonist-stimulated $[Ca^{2+}]_i$ oscillations regulate transcription and gene expression through CSD and $[Ca^{2+}]_i$ spike amplitude.

EXPERIMENTAL PROCEDURES

Cell Culture and $[Ca^{2+}]_i$ Measurements—The isolation and maintenance of human umbilical vein endothelial cells

* This work was supported by Research Grants 30971162, 81170048, 30900750, 31270031, and 30900545 from the National Natural Science Foundation of China, New Teacher Grant 20090142120015 from the Ministry of Education of China, and a Student Research Award from Tongji Medical College, Huazhong Science and Technology University (to Q. X. and C. L.).
[S] This article contains supplemental Figs. S1–S4.
[1] Both authors contributed equally to this work.
[2] To whom correspondence should be addressed: Dept. of Pathophysiology, Tongji Medical College, HUST, Wuhan 430030, People's Republic of China. Tel: 27-6331-4909; Fax: 027-8369-2608; E-mail: qinghuaa@mails.tjmu.edu.cn.

(HUVECs)[3] in culture (19) and $[Ca^{2+}]_i$ measurements were performed as described before (19, 20).

$[Ca^{2+}]_i$ Clamp and Determination of $[Ca^{2+}]_i$ Thresholds for NFκB and STAT3 Activation—Fura-2-loaded HUVECs on coverslips in the perfusion chamber were placed on the stage of a modified Olympus Diaphot inverted microscope. $[Ca^{2+}]_i$ was clamped using a computer-controlled solenoid valve (General Valve) perfusion system as described previously (19, 20). The $[Ca^{2+}]_i$ kinetics were controlled by varying exposure time of Ca^{2+}-containing and Ca^{2+}-free/EGTA buffer through the valve.

$[Ca^{2+}]_i$ oscillations were generated at a frequency of 0.6 min^{-1} with four different spike amplitudes of ~150, 190, 350, and 450 nM, respectively. To determine $[Ca^{2+}]_i$ thresholds for NFκB and STAT3 activation by $[Ca^{2+}]_i$ oscillations, HUVECs were exposed to the conditions that generated the above $[Ca^{2+}]_i$ oscillations in the presence of 10 μM histamine. Then cell lysates were prepared for subsequent ELISA-based determination of endogenous NFκB and STAT3 transcriptional activity (19, 20).

Simultaneous Monitoring of $[Ca^{2+}]_i$ and NFκB or STAT3 Nuclear Translocation—HUVECs grown to ~70% confluence on 24-mm-diameter circular glass coverslips were transfected with plasmid expressing RelA-EGFP or STAT3-EGFP (Clontech). Before the experiments, HUVECs were loaded with 1 μM Fura Red/AM in saline at 37 °C for 25 min and then allowed to deesterify at the same temperature for 25 min. The cells were stimulated by 10 μM histamine for 1 h, and the fluorescence imagings of Fura Red and EGFP were collected simultaneously through dual-channel confocal scanning (Olympus 1X71) by excitation at 543 nm and emission through a 610-nm long pass filter or excitation at 488 nm and emission through a 505–525-nm band pass filter for Fura Red and EGFP (21, 22), respectively. The long pass emission filtering of the Fura Red signal in an EGFP-expressing HUVEC sufficiently eliminated the EGFP-Fura Red emission spectra overlap and allowed quantitative calibration of $[Ca^{2+}]_i$ as employed previously (22). In separate experiments in control HUVECs, vector transfection showed no effect on histamine-stimulated $[Ca^{2+}]_i$ oscillations.

Data were analyzed using Fluoview v.5.0 by exporting mean fluorescence intensity of Fura Red from the whole of the cell as *F*. To calculate $[Ca^{2+}]_i$ (23, 24), the fluorescence achieved after high Ca^{2+} solution was designated as F_{max}, and the fluorescence obtained after zero Ca^{2+} solution as F_{min}. For a given fluorescence *F*, $[Ca^{2+}]_i = ((F - F_{min})/(F_{max} - F)) * K_D$ (K_D = 145 nM) (25). Actual single-spike duration was measured at $[Ca^{2+}]_i$ of 180 and 395 nM, the threshold $[Ca^{2+}]_i$ level for NFκB and STAT3 activation by $[Ca^{2+}]_i$ oscillations, respectively. The CSD was obtained by adding the single-spike duration of each $[Ca^{2+}]_i$ spike during oscillations. The mean fluorescence intensity of GFP was exported from the whole of cytoplasm or nucleus for each cell and the translocation of NFκB or STAT3 were expressed as a normalized nucleus to cytoplasm ratio.

[3] The abbreviations used are: HUVEC, human umbilical vein endothelial cell; CSD, cumulative spike duration; CV, coefficient of variations; EGFP, enhanced GFP.

Measurement of Endogenous NFκB and STAT3 Transcriptional Activity—An ELISA-based assay was performed to measure endogenous NFκB activities in HUVECs using the modified procedure with greatly improved sensitivity and specificity that we recently established (19, 20, 26). Briefly, treated HUVECs were lysed with lysis buffer (20 mM HEPES, pH 7.5, 0.35 M NaCl, 20% glycerol, 1% Nonidet P-40, 1 mM $MgCl_2 \cdot 6H_2O$, 0.5 mM EDTA, 0.1 mM EGTA) containing a protease inhibitor mixture (Calbiochem) on ice for 10 min. The supernatant obtained after centrifugation at 14,000 rpm for 30 min at 4 °C constituted the total protein extract and was recovered and stored at −80 °C. The double-stranded probe with single-stranded linker was generated by a 1:1 mix of the following two oligonucleotide with the sequences of 5′-AGTTGAG*GGG*ACTTTCCCAGGCC-(^{34}C)-C-3′, the 3′-end biotinylated, and 5′-GCCTGGGAAAG-TCCCCTCAACT-3′; or 5′-CATTTCCCGTAAATCC(^{34}C)-C-3′, the 3′-end is biotinylated and 5′-GGATTTACGGGAA-ATG-3′ for NFκB and STAT3, respectively. The probe was denatured at 94 °C for 10 min, annealed at room temperature overnight, and then linked to streptavidin-coated 96-well plates (Roche Applied Bioscience) by incubating 2 pmol of probe per well for 1 h at 37 °C in 50 μl of phosphate-buffered saline (PBS). After the wash, 20 μl of cell extract was mixed with 30 μl of binding buffer (4 mM HEPES, pH 7.5, 100 mM KCl, 8% glycerol, 5 mM DTT, 0.2% BSA, 40 μg/ml salmon sperm DNA) in the above microwells incubated at room temperature with mild agitation (200 rpm) for 1 h. After washing, mouse anti-NFκB p65 or anti-STAT3 monoclonal antibody (diluted 1:1000; Santa Cruz Biotechnology) was incubated for 1 h at room temperature. After washing, peroxidase-conjugated goat anti-mouse IgG (diluted 1:1000; Santa Cruz Biotechnology) was incubated at room temperature for 1 h. After washing, 100 μl of tetramethylbenzidine was incubated at room temperature for 10 min before adding 100 μl of stopping solution (2 M H_2SO_4). Optical density was then read at 450 nm under a microplate reader (TECAN, Austria) using a 655-nm reference wavelength. Backgrounds were determined in lysis buffer and subtracted before data analysis.

Western Blot Analysis of IκB-α and JAK2 Phosphorylation—Western blotting was performed as we described recently (27). Briefly, protein extracts were separated on SDS-polyacrylamide minigels and transferred onto nitrocellulose membranes, blocked with PBS containing 5% nonfat dried milk for 1 h at room temperature, and incubated at 4 °C overnight with antibodies for phosphorylated IκB-α or JAK2 and β-actin (Santa Cruz Biotechnology) in PBS containing 5% nonfat dried milk and 0.1% Tween 20. The secondary peroxidase-conjugated anti-mouse IgG was incubated for 1 h at room temperature. Blots were washed with PBS and developed using enhanced chemiluminescence detection reagents (Thermo Scientific) following the manufacturer's instructions. The phosphorylated IκB-α (~41 kDa) or JAK2 (90–132 kDa) was quantified using an imaging densitometer (G860B; Epson) and normalized by β-actin.

Assessment of IL-8 and VEGF mRNA Expression by Real-time RT-PCR—Total RNA was isolated from treated HUVECs and subject to real-time PCR as described previously (19). Briefly, 1 μg of total RNA for each sample was used to generate cDNA

using Superscript First Strand System (Takara). Each RNA/primer was gently mixed with 20 μl of cDNA Synthesis Mix (Takara) and incubated at 37 °C for 15 min. The reactions were terminated by a 5-min incubation at 85 °C and then chilled on ice. Real-time PCR was performed on Rotor Gene 3000 (Corbett) using Sybgree1 Mix (Takara) and specific primers for IL-8 or VEGF and β-actin from Invitrogen. The thermal cycle conditions were 10 s at 95 °C and a 40-cycle loop: 5 s at 95 °C and 20 s at 60 °C. The standard curve for each gene was generated and used to quantify the mRNA concentration of each sample. Duplicate measurements were conducted, and the IL-8 and VEGF mRNA level was normalized by β-actin and then expressed as a -fold of the corresponding control for each condition.

Statistical Analysis—Data are reported as mean ± S.E. Statistical comparisons were made using one-way ANOVA followed by a Holm-Sidak test. The two-parameter power regression, four-parameter logistic regression or hyperbola curve was used for nonlinear regression. A difference was considered significant at $p < 0.05$.

RESULTS

Agonist-stimulated Irregular $[Ca^{2+}]_i$ Oscillations—Histamine-stimulated $[Ca^{2+}]_i$ oscillations in 112 of a total 203 cells examined from seven separate experiments. In each of the remaining cells, a single $[Ca^{2+}]_i$ spike was noted. $[Ca^{2+}]_i$ oscillated with varied parameters, the coefficients of variations (CVs) were 51.05 ± 1.83%, 34.21 ± 3.70%, and 28.16 ± 1.64% for amplitude, spike duration, and interspike interval, respectively. The CVs of these parameters were significant different from those of regular $[Ca^{2+}]_i$ oscillation models employed in our previous studies in this type of cells ($p < 0.05$ *versus* CVs of 7.11 ± 0.53%, 8.15 ± 0.56%, and 15.73 ± 1.14%, $n = 32$ for amplitude, spike duration, and interspike interval of regular $[Ca^{2+}]_i$ oscillations models, respectively (20). In hepatocytes, the CV of interspike intervals induced by noise was considered to be in the range of 10–15% (28, 29), highly coinciding with ours in regular $[Ca^{2+}]_i$ oscillations models (20). Thus, the minimal CV at 15% in the interspike interval can be used as the threshold to separate $[Ca^{2+}]_i$ oscillations into irregular and regular ones. Accordingly, histamine-stimulated $[Ca^{2+}]_i$ oscillations in the current study were irregular in >80% of the cells. Because interspike interval was the one with least CV among the above parameters, histamine-stimulated $[Ca^{2+}]_i$ oscillations were generally irregular in the current study. In 100 (>89%) of a total 112 cells showing $[Ca^{2+}]_i$ oscillations, histamine induced irregular parameters with decreasing spike amplitude, decreasing spike duration and increasing interspike intervals.

Determination of $[Ca^{2+}]_i$ Thresholds for NFκB and STAT3 Activation—To determine $[Ca^{2+}]_i$ thresholds for NFκB and STAT3 activation by $[Ca^{2+}]_i$ oscillations, HUVECs were exposed to the conditions that generated the 0.6 min^{-1} frequent $[Ca^{2+}]_i$ oscillations with four different spike amplitudes of ~150, 190, 350, and 450 nM, respectively, in the presence of 10 μM histamine. Then, cell lysates were assayed for endogenous NFκB and STAT3 transcriptional activity. As shown in Fig. 1, regression analysis and forecasting determined $[Ca^{2+}]_i$ thresholds to be ~180 nM and 395 nM for NFκB and STAT3 activation by $[Ca^{2+}]_i$ oscillations in HUVECs, respectively. These results also imply that amplitude is one candidate for the possible parameter(s) in determining $[Ca^{2+}]_i$ oscillations-encoded transcription.

CSD- and Spike Amplitude-regulated Transcription Correlation Revealed in Single-cell Studies—To reveal the dynamic regulation of transcriptional activation by $[Ca^{2+}]_i$ oscillations, cells transfected with RelA-GFP or STAT3-GFP vector were loaded with Fura Red and then subjected to a stimulation of 10 μM histamine for 60 min. Alterations in $[Ca^{2+}]_i$ and GFP translocation in each individual cell were simultaneously monitored as shown in Fig. 2, *a* and *b* (for RelA). In a total of 164 cells examined in 61 separate experiments for NFκB, $[Ca^{2+}]_i$ spike amplitude in 80 of 112 cells showing $[Ca^{2+}]_i$ oscillations and in 40 of 52 showing a single $[Ca^{2+}]_i$ transient reached a level of ≥180 nM, the $[Ca^{2+}]_i$ threshold level for NFκB transcriptional activation in this type of cells (Fig. 1). Single-spike duration at the $[Ca^{2+}]_i$ level of 180 nM, $[Ca^{2+}]_i$ oscillation frequency, and CSD (also at the $[Ca^{2+}]_i$ level of 180 nM) as well as averaged spike amplitude of each cell were determined individually and plotted against the ratio of nucleus/cytosol NFκB-GFP fluorescent intensity for each cell (Fig. 2, c_i–f_i). The significant regression did not fit between $[Ca^{2+}]_i$ oscillation frequency or single-spike duration and NFκB translocation ($p > 0.05$, Fig. 2, c_i and d_i, respectively); however, it fit well between averaged spike amplitude and NFκB translocation as well as between CSD and NFκB translocation (four parameter logistic regression, $p < 0.05$, Fig. 2, e_i and f_i, respectively). To reveal more details about the significant correlation between CSD and NFκB translocation, cells with $[Ca^{2+}]_i$ oscillations were separated by their frequencies. For each of the 0.1, 0.2, and 0.3 min^{-1} frequent $[Ca^{2+}]_i$ oscillations, CSD dynamically regulated NFκB translocation for cells with the same frequency (four-parameter logistic regression, $n = 22$, 27, and 22 cells, $p < 0.05$ for 0.1, 0.2, and 0.3 min^{-1} frequency as in supplemental Fig. S1, a_i–a_{iii}, respectively). Cells with $[Ca^{2+}]_i$ oscillations were also separated by their CSDs in the narrow ranges that did not significantly affect NFκB translocation. For each of the 90–190, 208–385, 394–445, 481–578, 635–812, and 853–1326-s CSDs, frequency did not correlate with NFκB translocation for cells within the narrow range of CSD ($n = 13$, 16, 12, 12, 11, and 16 cells, $p > 0.05$ for 90–190, 208–385, 394–445, 481–578, 635–812, and 853–1326 s as in supplemental Fig. S1, b_i–b_{vi}, respectively). In a total of 271 cells examined in 40 separate experiments for STAT3, $[Ca^{2+}]_i$ spike amplitudes in 97 of 157 cells showing $[Ca^{2+}]_i$ oscillations and in 58 of 114 cells showing a single $[Ca^{2+}]_i$ transient reached a level of ≥395 nM, the $[Ca^{2+}]_i$ threshold level for STAT3 transcriptional activation in this type of cells (supplemental Fig. S1). Being consistent with NFκB, the significant regression did not fit between $[Ca^{2+}]_i$ oscillation frequency or single-spike duration and STAT3 translocation ($p > 0.05$, Fig. 2, c_{ii} and d_{ii}, respectively); however, it fit well between averaged spike amplitude and STAT3 translocation as well as between CSD and STAT3 translocation (two-parameter power regression, $p < 0.05$, Fig. 2, e_{ii} and f_{ii}, respectively). Also being consistent with NFκB, for each of the 0.1, 0.2, and 0.3 min^{-1} frequent $[Ca^{2+}]_i$ oscillations, CSD dynamically regulated STAT3

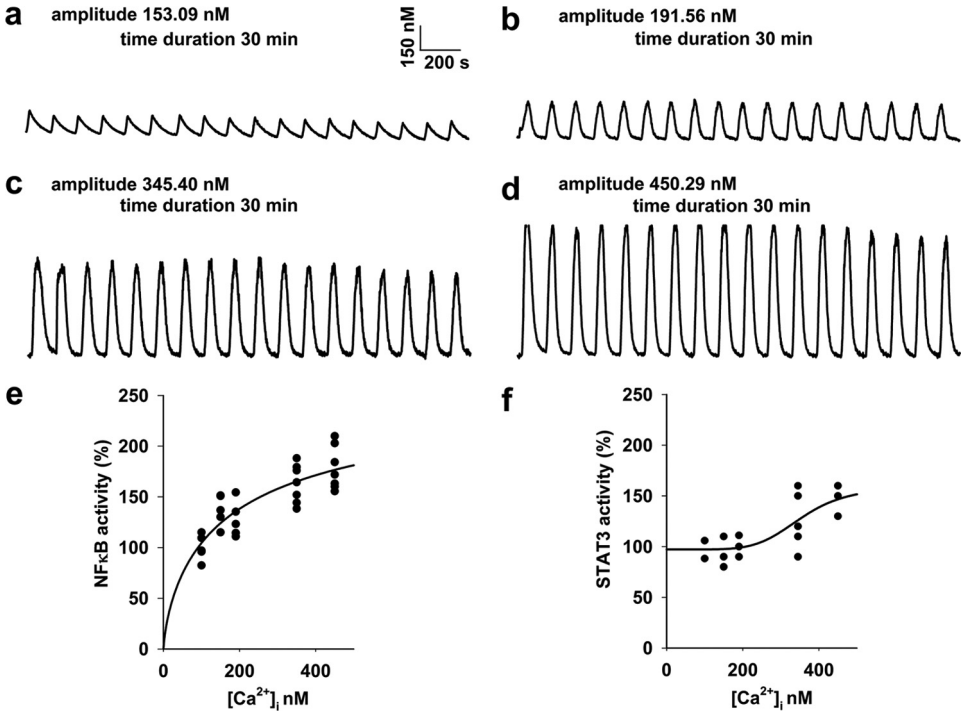

FIGURE 1. **Determination of $[Ca^{2+}]_i$ thresholds for NFκB and STAT3 activation by $[Ca^{2+}]_i$ oscillations.** $[Ca^{2+}]_i$ oscillations were generated in cell monolayers at a frequency of 0.6 min^{-1} with four different spike amplitudes of 153.09 ± 3.23, 191.73 ± 3.00, 345.40 ± 10.91, and 450.29 ± 8.51 nM as in *a*, *b*, *c*, and *d*, respectively ($n = 20–86$ cells from 3–4 separate experiments for each). To determine $[Ca^{2+}]_i$ thresholds for NFκB and STAT3 activation by $[Ca^{2+}]_i$ oscillations, cell monolayers were exposed to the conditions that generated the $[Ca^{2+}]_i$ oscillations as *a*, *b*, *c*, and *d* for 30 min, respectively. Then cell lysates were prepared for subsequent ELISA for the measurement of endogenous NFκB and STAT3 transcriptional activities. Regression analysis and forecasting determined $[Ca^{2+}]_i$ thresholds to be 180 and 395 nM for NFκB and STAT3 activation by $[Ca^{2+}]_i$ oscillations, respectively (four-parameter logistic regression, $p < 0.05$, $n = 3–7$ separate experiments for *e* and *f*).

translocation for cells with the same frequency (two-parameter power regression, $n = 32$, 34, and 17 cells, $p < 0.05$ for 0.1, 0.2, and 0.3 min^{-1} frequency as in supplemental Fig. S2, $a_i–a_{iii}$, respectively); for each of the 21–100, 102–195, 204–297, 301–389, and 405–537-s CSDs, frequency did not correlate with STAT3 translocation for cells within the narrow range of CSD ($n = 30$, 21, 21, 12, and 13 cells, $p > 0.05$ for 21–100, 102–195, 204–297, 301–389, and 405–537 s as in supplemental Fig. S2, $b_i–b_v$, respectively). Thus, the transcriptional activities of NFκB and STAT3 are stimulated by agonists to different levels by the same frequent $[Ca^{2+}]_i$ oscillations with different CSDs or to the similar levels by the different frequent $[Ca^{2+}]_i$ oscillations with the similar CSDs.

CSD-regulated Transcription Cause-Effect Confirmed in Cell Population Studies—To confirm the importance of CSD in regulation of transcription as revealed by their significant correlations in single-cell experiments, homogeneous $[Ca^{2+}]_i$ oscillations were generated in cell monolayers mimicking the predominant pattern of histamine-induced irregular $[Ca^{2+}]_i$ oscillations with decreasing spike amplitude, decreasing spike duration, and increasing interspike intervals. $[Ca^{2+}]_i$ oscillations were generated by alternately exposing intracellular Ca^{2+} store-depleted cell monolayers to Ca^{2+}-free or Ca^{2+}-containing buffer in the presence of 10 μM histamine (19, 20) at a frequency of 0.6 min^{-1} with two different CSDs of 1215.63 ± 31.25 and 1748.48 ± 27.02 s at the $[Ca^{2+}]_i$ level of 180 nM for NFκB, while with the same CSDs of 185.49 ± 7.33 and 200.47 ± 20.61 s at the $[Ca^{2+}]_i$ level of 395 nM for STAT3 as shown in Fig. 3, *a* and *b*, respectively. $[Ca^{2+}]_i$ oscillations were also generated at a frequency of 0.3 min^{-1} with different CSDs of 649.73 ± 16.95 and 1127.38 ± 13.34 s for NFκB, while with the same CSDs of 201.35 ± 13.68 and 216.93 ± 13.80 s for STAT3, as well as at a frequency of 0.2 min^{-1} with different CSDs of 458.02 ± 11.32 and 769.05 ± 20.51 s for NFκB, while with the same CSDs of 172.50 ± 7.49 and 208.15 ± 11.39 s for STAT3, as Fig. 3, *d*, *e*, *g*, and *h*, respectively. Cell monolayers were exposed to the conditions that generated the $[Ca^{2+}]_i$ oscillations as *a*, *b*, *d*, *e*, *g*, and *h* for 70 min, respectively. Then cell lysate were prepared for subsequent ELISA for determination of endogenous NFκB and STAT3 transcriptional activity (20). For $[Ca^{2+}]_i$ oscillations with 0.2, 0.3, or 0.6 min^{-1} frequency and different CSDs for NFκB, the induced NFκB activities were different, as Fig. 3, c_i, f_i, and i_i ($p < 0.05$, $n = 4–18$ for each), respectively. For $[Ca^{2+}]_i$ oscillations with 0.2, 0.3, and 0.6 min^{-1} frequency and the same CSDs for STAT3, the induced STAT3 activities were not different, as in Fig. 3, c_{ii}, f_{ii}, and i_{ii} (p = not significant, $n = 4–18$ for each), respectively.

To consolidate the importance of CSD in regulation of NFκB and STAT3 transcription, homogeneous $[Ca^{2+}]_i$ oscillations were further generated in cell monolayers in the presence of 10 μM histamine (19, 20) at frequencies of 0.6 min^{-1} and 0.3 min^{-1} with the same CSDs of 1215.63 ± 31.25 and 1219.79 ± 10.34 s at the $[Ca^{2+}]_i$ level of 180 nM for NFκB, and with the same CSDs of 185.49 ± 7.33 and 196.05 ± 3.39 s at the $[Ca^{2+}]_i$ level of 395 nM for STAT3 as Fig. 4, *a* and *b*, respectively. $[Ca^{2+}]_i$ oscillations were also generated at frequencies of 0.3 min^{-1} and 0.2 min^{-1} with the same CSDs of 649.73 ± 16.95 and 659.05 ± 20.51 s for NFκB and with the same CSDs of 201.35 ± 13.68 and

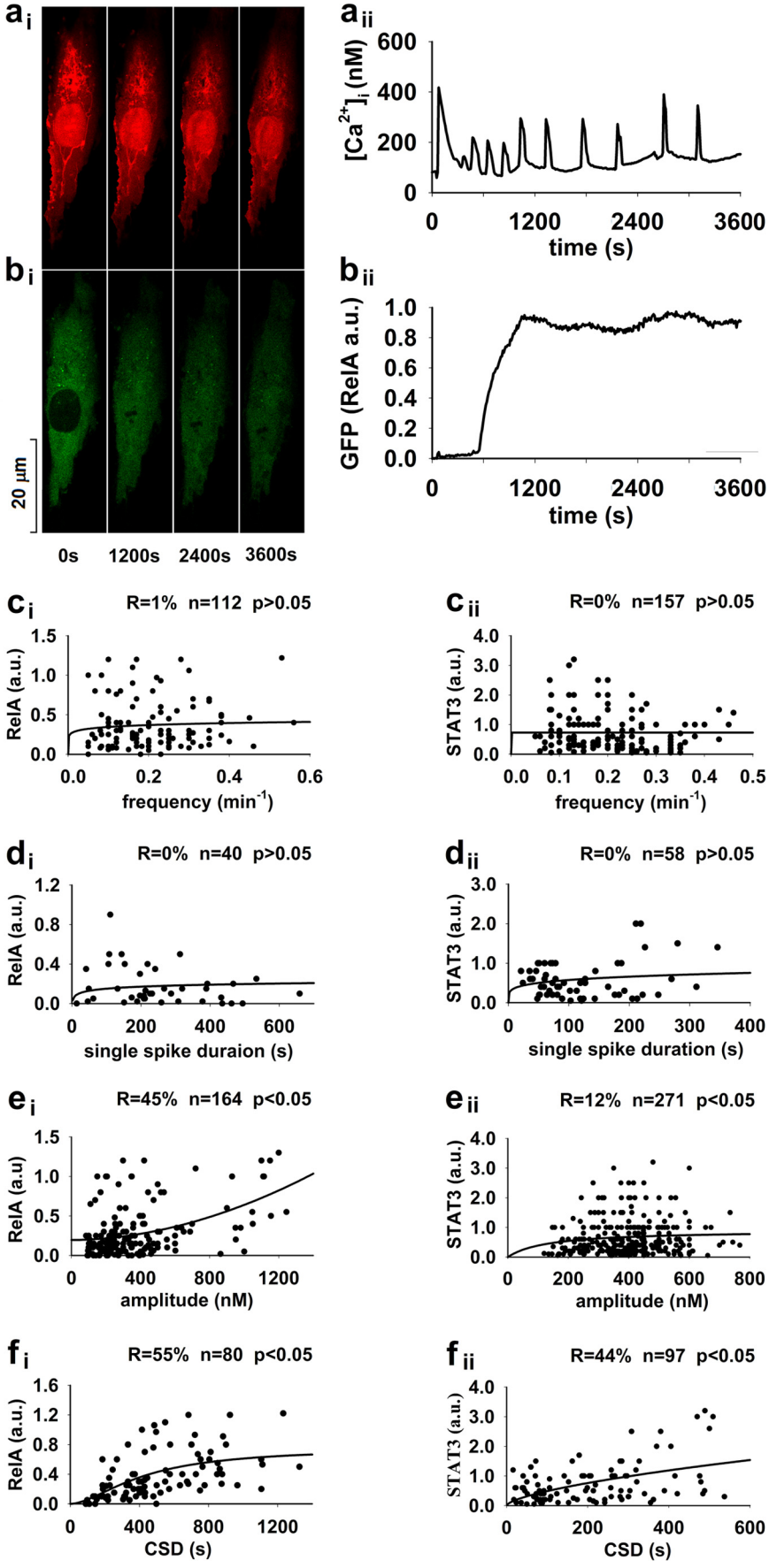
a i
a ii
[Ca2+]i (nM)
600
400
200
0
0
1200
2400
3600
time (s)
b i
b ii
GFP (RelA a.u.)
1.0
0.8
0.6
0.4
0.2
0.0
0
1200
2400
3600
time (s)
20 µm
0s
1200s
2400s
3600s
c i
R=1% n=112 p>0.05
RelA (a.u.)
frequency (min-1)
c ii
R=0% n=157 p>0.05
STAT3 (a.u.)
frequency (min-1)
d i
R=0% n=40 p>0.05
RelA (a.u.)
single spike duraion (s)
d ii
R=0% n=58 p>0.05
STAT3 (a.u.)
single spike duration (s)
e i
R=45% n=164 p<0.05
RelA (a.u)
amplitude (nM)
e ii
R=12% n=271 p<0.05
STAT3 (a.u.)
amplitude (nM)
f i
R=55% n=80 p<0.05
RelA (a.u.)
CSD (s)
f ii
R=44% n=97 p<0.05
STAT3 (a.u.)
CSD (s)

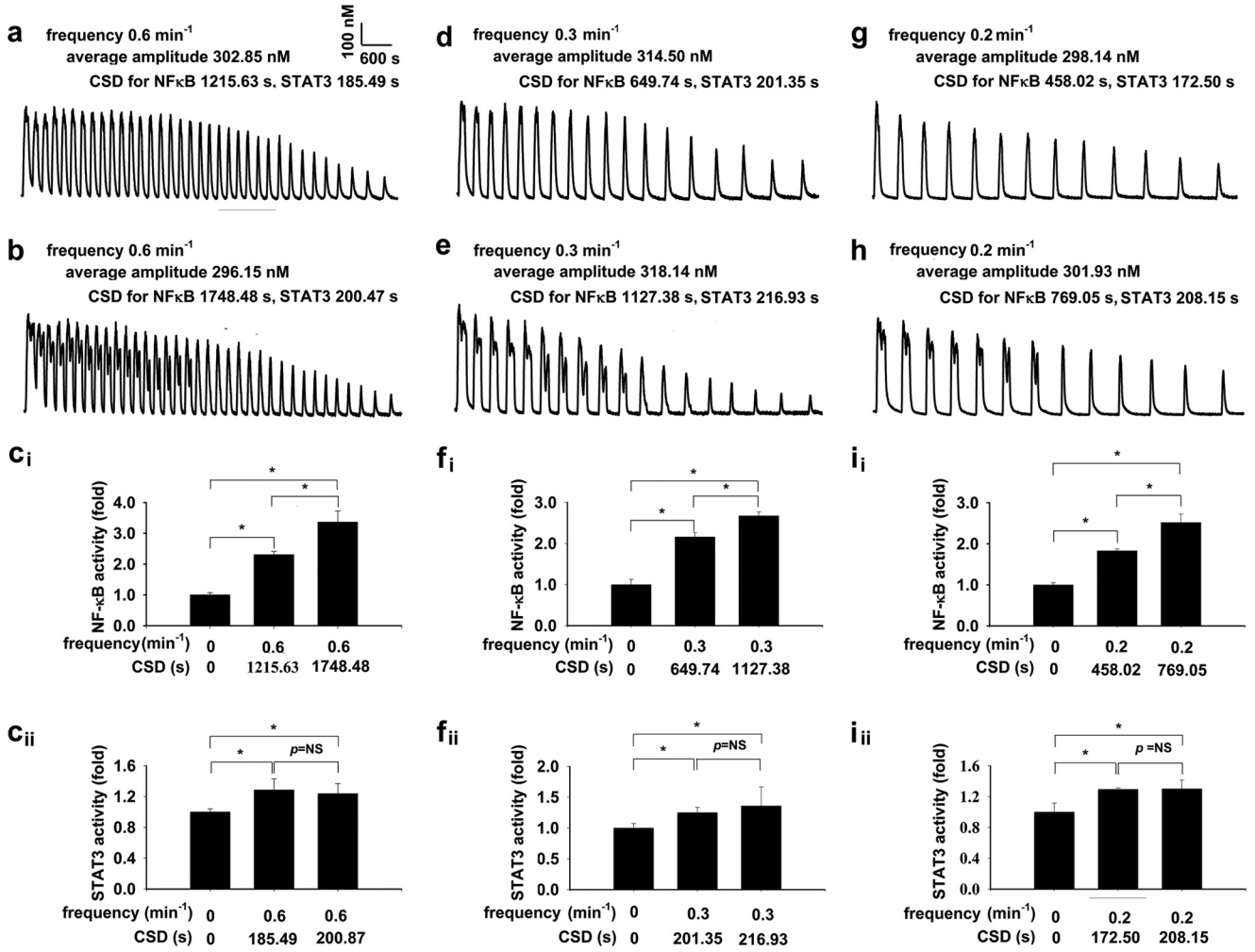

FIGURE 3. **CSD regulates endogenous NFκB and STAT3 transcriptional activities by irregular $[Ca^{2+}]_i$ oscillations in cell monolayers-I.** $[Ca^{2+}]_i$ oscillations were generated in cell monolayers mimicking the predominant pattern of histamine-induced irregular $[Ca^{2+}]_i$ oscillations with decreasing spike amplitude, decreasing spike duration, and increasing interspike intervals. $[Ca^{2+}]_i$ oscillations were generated in the presence of 10 μM histamine at a frequency of 0.6 min^{-1} with two different CSDs of 1215.63 ± 31.25 and 1748.48 ± 27.02 s at the $[Ca^{2+}]_i$ level of 180 nM for NFκB, while with the same CSDs of 185.49 ± 7.33 and 200.47 ± 20.61 s at the $[Ca^{2+}]_i$ level of 395 nM for STAT3 as *a* and *b*, respectively. $[Ca^{2+}]_i$ oscillations were also generated at a frequency of 0.3 min^{-1} with different CSDs of 649.73 ± 16.95 and 1127.38 ± 13.34 s for NFκB, while with the same CSDs of 201.35 ± 13.68 and 216.93 ± 13.80 s for STAT3, as well as at a frequency of 0.2 min^{-1} with different CSDs of 458.02 ± 11.32 and 769.05 ± 20.51 s for NFκB, while with the same CSDs of 172.50 ± 7.49 and 208.15 ± 11.39 s for STAT3, as in *d*, *e*, *g*, and *h*, respectively. Cell monolayers were exposed to the conditions that generated the $[Ca^{2+}]_i$ oscillations as in *a*, *b*, *d*, *e*, *g*, and *h* for 70 min, respectively. Then cell lysate were prepared for a subsequent ELISA for determination of endogenous NFκB and STAT3 transcriptional activity. For $[Ca^{2+}]_i$ oscillations with 0.2, 0.3, or 0.6 min^{-1} frequencies and different CSDs for NFκB, the induced NFκB activities were different, as c_i, f_i, and i_i (*, $p < 0.05$, $n = 4–18$). For $[Ca^{2+}]_i$ oscillations with 0.2, 0.3, and 0.6 min^{-1} frequencies and the same CSDs for STAT3, the induced STAT3 activities were not different, as in c_{ii}, f_{ii}, and i_{ii} (p = not significant (*NS*), $n = 4–18$).

207.26 ± 9.23 s for STAT3, as in Fig. 4, *d* and *e*, respectively. Cell monolayers were exposed to the conditions that generated the $[Ca^{2+}]_i$ oscillations as Fig. 4, *a*, *b*, *d*, and *e*, for 70 min, respectively. For $[Ca^{2+}]_i$ oscillations with 0.3 and 0.6 min^{-1} frequencies or 0.3 and 0.2 min^{-1} frequencies and the same CSDs for NFκB, the induced NFκB activities were similar, as in Fig. 4, c_i and f_i (p = not significant, $n = 4–18$ for each), respectively. For $[Ca^{2+}]_i$ oscillations with 0.3 and 0.6 min^{-1} frequencies or 0.3 and 0.2 min^{-1} frequencies and the same CSDs for STAT3, the induced STAT3 activities were not different, as shown in Fig. 4, c_{ii} and f_{ii} (p = not significant, $n = 4–18$ for each), respectively.

FIGURE 2. **CSD and spike amplitude correlate with nuclear translocation of NFκB and STAT3 in histamine-stimulated single cell(s).** Representative real-time fluorescent images of a cell show simultaneous measurements of Fura Red Ca^{2+} fluorescence (*red*, a_i) and GFP (RelA) translocation from cytosol to nucleus (*green*, b_i) before and after a 60-min stimulation of 10 μM histamine and time course alterations in $[Ca^{2+}]_i$ (a_{ii}) and the ratio of nucleus/cytosol GFP (RelA) fluorescence intensity (b_{ii}). For NFκB (c_i–f_i), in a total of 164 cells examined in 61 separate experiments, $[Ca^{2+}]_i$ spike amplitude in 80 of 112 cells showing $[Ca^{2+}]_i$ oscillations and in 40 of 52 cells showing a single $[Ca^{2+}]_i$ transient reached a level of ≥180 nM, the $[Ca^{2+}]_i$ threshold level for NFκB activation in the current study. For STAT3 (c_{ii}–f_{ii}), in a total of 271 cells examined in 40 separate experiments, $[Ca^{2+}]_i$ spike amplitude in 97 of 157 cells showing $[Ca^{2+}]_i$ oscillations and in 58 of 114 cells showing a single $[Ca^{2+}]_i$ transient reached a level of ≥395 nM, the $[Ca^{2+}]_i$ threshold level for STAT3 transcriptional activation in the current study. The significant regression did not fit between $[Ca^{2+}]_i$ oscillation frequency or single-spike duration and nuclear translocation of transcriptional factors ($p > 0.05$, c_i–d_i and c_{ii}-d_{ii} for NFκB or STAT3, respectively); however, it fit well between averaged spike amplitude and nuclear translocation of transcriptional factors as well as between CSD and nuclear translocation of transcriptional factors (four-parameter logistic regression, $p < 0.05$, e_i and f_i for NFκB; two-parameter power regression, $p < 0.05$, e_{ii} and f_{ii} for STAT3, respectively).

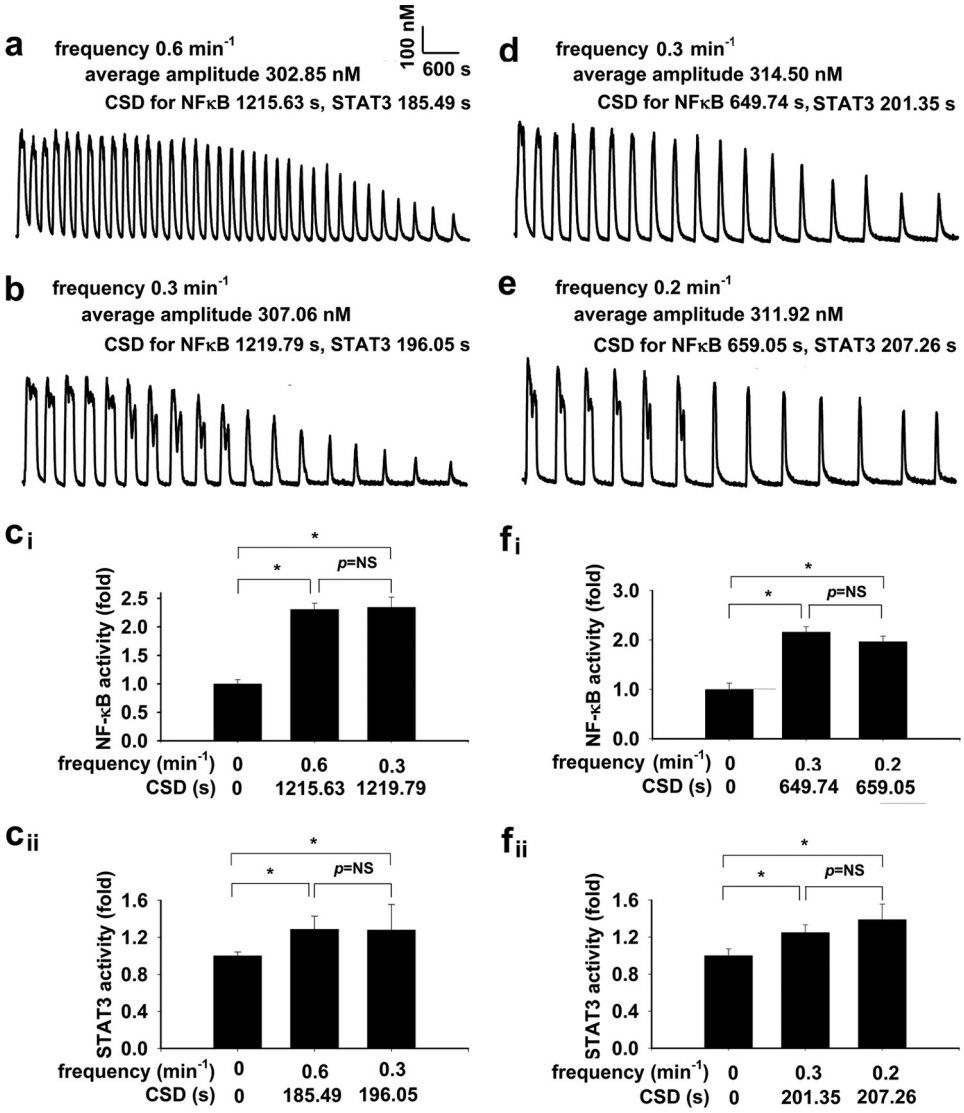

FIGURE 4. **CSD regulates endogenous NFκB and STAT3 transcriptional activities by irregular $[Ca^{2+}]_i$ oscillations in cell monolayers-II.** $[Ca^{2+}]_i$ oscillations were further generated in cell monolayers in the presence of 10 μM histamine at frequencies of 0.6 min^{-1} and 0.3 min^{-1} with the same CSDs of 1215.63 ± 31.25 and 1219.79 ± 10.34 s at the $[Ca^{2+}]_i$ level of 180 nM for NFκB, and with the same CSDs of 185.49 ± 7.33 and 196.05 ± 3.39 s at the $[Ca^{2+}]_i$ level of 395 nM for STAT3 as in *a* and *b*, respectively. $[Ca^{2+}]_i$ oscillations were also generated at frequencies of 0.3 min^{-1} and 0.2 min^{-1} with the same CSDs of 649.73 ± 16.95 and 659.05 ± 20.51 s for NFκB, and with the same CSDs of 201.35 ± 13.68 and 207.26 ± 9.23 s for STAT3, as in *d* and *e*, respectively. Cell monolayers were exposed to the conditions that generated the $[Ca^{2+}]_i$ oscillations as in *a*, *b*, *d*, and *e* for 70 min, respectively, and the subsequent ELISA determined endogenous NFκB and STAT3 activities. For $[Ca^{2+}]_i$ oscillations with 0.3 and 0.6 min^{-1} frequencies or 0.3 and 0.2 min^{-1} frequencies and the same CSDs for NFκB, the induced NFκB activities are similar, as in c_i and f_i (p = not significant (*NS*), n = 4–18). For $[Ca^{2+}]_i$ oscillations with 0.3 and 0.6 min^{-1} frequencies or 0.3 and 0.2 min^{-1} frequencies and the same CSDs for STAT3, the induced STAT3 activities are not different, as in c_{ii} and f_{ii} (p = NS, n = 4–18).

CSD-regulated Transcription: Mechanism and Significance—To reveal the mechanism underlying CSD-regulated transcriptional activation, cells were subjected to conditions that generated irregular $[Ca^{2+}]_i$ oscillations in the presence of 10 μM histamine (19, 20) with the same frequency and different CSD or with the different frequencies and the same CSD for NFκB. For STAT3, these irregular $[Ca^{2+}]_i$ oscillations had the similar CSD. The phosphorylated IκB-α were stimulated to different levels by the 0.3 min^{-1} $[Ca^{2+}]_i$ oscillations with different CSDs, or to the same level by the 0.3 min^{-1} and 0.2 min^{-1} $[Ca^{2+}]_i$ oscillations with the same CSD ($p < 0.05$, $n = 3–4$ for each, Fig. 5a_i). The phosphorylated JAK2 were stimulated to the same level by the 0.3 min^{-1} $[Ca^{2+}]_i$ oscillations with the similar CSDs, or to the same level by the 0.3 min^{-1} and 0.2 min^{-1} $[Ca^{2+}]_i$ oscillations with the same CSD ($p < 0.05$, $n = 3–4$ for each, Fig. 5a_{ii}).

To reveal the biological consequence from CSD-regulated transcriptional activation, experiments employing the same strategies as for IκB-α and JAK2 were conducted in cell monolayers. The mRNA expression of interleukin-8 (IL-8), a known NFκB-dependent gene, was stimulated to different levels by the 0.3 min^{-1} $[Ca^{2+}]_i$ oscillations with different CSDs, or to the same level by the 0.3 min^{-1} and 0.2 min^{-1} $[Ca^{2+}]_i$ oscillations with the same CSD ($p < 0.05$, $n = 3–4$ for each, Fig. 5b_i). The VEGF mRNA, a STAT3-dependent gene, was stimulated to the same level by the 0.3 min^{-1} $[Ca^{2+}]_i$ oscillations with the similar CSDs, or to the same level by the 0.3 min^{-1} and 0.2 min^{-1} $[Ca^{2+}]_i$ oscillations with the same CSD (*, $p < 0.05$, $n = 3–4$ for each, Fig. 5b_{ii}).

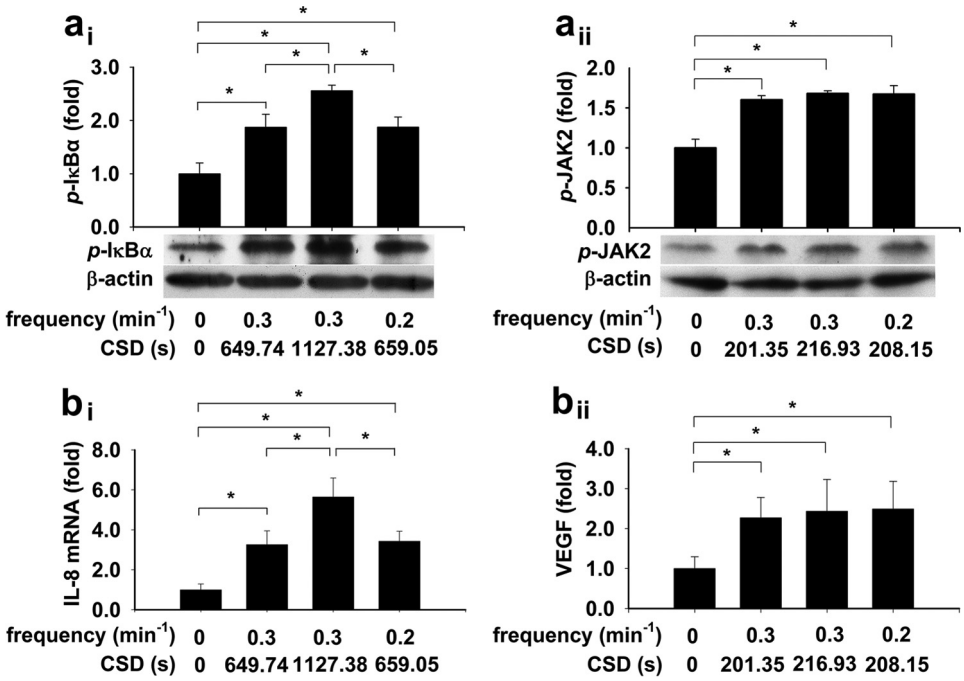

FIGURE 5. **CSD regulates IκB-α and JAK2 phosphorylation, IL-8, and VEGF gene expression induced by irregular $[Ca^{2+}]_i$ oscillations.** Cell monolayers were subjected to conditions that generated irregular $[Ca^{2+}]_i$ oscillations in the presence of 10 μM histamine with the same frequency and different CSDs or with the different frequencies and the same CSD for NFκB. For STAT3, these irregular $[Ca^{2+}]_i$ oscillations had similar CSDs. The phosphorylated IκB-α were stimulated to different levels by the 0.3 min^{-1} $[Ca^{2+}]_i$ oscillations with different CSDs, or to the same level by the 0.3 min^{-1} and 0.2 min^{-1} $[Ca^{2+}]_i$ oscillations with the same CSD (*, $p < 0.05$, $n = 3–4$ for each, a_i). The phosphorylated JAK2 are stimulated to the same level by the 0.3 min^{-1} $[Ca^{2+}]_i$ oscillations with the similar CSDs, or to the same level by the 0.3 min^{-1} and 0.2 min^{-1} $[Ca^{2+}]_i$ oscillations with the same CSD (*, $p < 0.05$, $n = 3–4$ for each, a_{ii}). The IL-8 mRNA are stimulated to different levels by the 0.3 min^{-1} $[Ca^{2+}]_i$ oscillations with different CSDs, or to the same level by the 0.3 min^{-1} and 0.2 min^{-1} $[Ca^{2+}]_i$ oscillations with the same CSD (*, $p < 0.05$, $n = 3–4$ for each, b_i). The VEGF mRNA are stimulated to the same level by the 0.3 min^{-1} $[Ca^{2+}]_i$ oscillations with the similar CSDs, or to the same level by the 0.3 min^{-1} and 0.2 min^{-1} $[Ca^{2+}]_i$ oscillations with the same CSD (*, $p < 0.05$, $n = 3–4$ for each, b_{ii}).

DISCUSSION

Irregular kinetics in $[Ca^{2+}]_i$ oscillations were even noted from the very beginning of documentations of $[Ca^{2+}]_i$ oscillations in literature (4, 5) and thereafter have been broadly or universally reported in a variety of cell types under various conditions, both within a given cell and between cells (6–15). Dynamic regulation of downstream events has been studied in $[Ca^{2+}]_i$ oscillation models mimicking regular ones only (17–20). In the studies using those models, $[Ca^{2+}]_i$ dynamics were artificially manipulated uniformly in cells to mimic regular $[Ca^{2+}]_i$ oscillations, however not irregular ones, the major pattern of really biologically relevant $[Ca^{2+}]_i$ oscillations. As a matter of fact, irregular ones induced by agonist stimulation, the predominant patterns in biologically relevant $[Ca^{2+}]_i$ oscillations, have never been explored experimentally.

Histamine-stimulated $[Ca^{2+}]_i$ oscillations with varied parameters in cells in the current study, representing irregular $[Ca^{2+}]_i$ oscillations. Irregularity and heterogeneity are the challenges for revealing dynamic regulation of downstream events by this kind of $[Ca^{2+}]_i$ oscillations. Therefore in the current study, our first experimental attempt was to simultaneously monitor and quantify $[Ca^{2+}]_i$ signal and NFκB/STAT3 translocation stimulated by histamine in each individual cell and the correlation between spike amplitude and CSD and the extent of NFκB/STAT3 translocation was revealed by regression analysis. The amplitude-dependent regulation of transcriptional activation of NFκB and STAT3 revealed in the current study is completely consistent with previous reports in $[Ca^{2+}]_i$ oscillation models dealing regular $[Ca^{2+}]_i$ oscillations (3, 17), and this is probably due to the low and high Ca^{2+} binding affinity of their upstream activator (3). In fact, the transcriptional factor of NFκB and STAT3 show as low as ~180 and high as ~350 nM $[Ca^{2+}]_i$ threshold for their activation in cells in the current experimental condition, respectively.

We realize that the limitation of correlation warrants experiments for logistical confirmation. To establish firmly the cause-and-effect relationships between CSD and NFκB/STAT3 transcription, the second experimental effort in the current study was to confirm the correlation using irregular $[Ca^{2+}]_i$ oscillation models mimicking the major pattern of histamine-stimulated irregular ones. Of note, what we actually employed in the current study was $[Ca^{2+}]_i$ oscillation models with manipulated parameters in the presence of agonist stimulation, a novel strategy we recently established that fully exploits the advantages of both membrane receptor occupation-stimulated $[Ca^{2+}]_i$ oscillations as physiological simulation and "artificially" generated $[Ca^{2+}]_i$ oscillations as manipulative parameters (19, 20).

The unexpected finding from experiments in single individual cells of the current study was the failure of frequency in regulating transcription of NFκB and STAT3. This seems different from the previous studies including ours showing that frequency widely regulated downstream events including transcriptional activation of NFκB and STAT3 (3, 17–20). In a most recent study, it was revealed that frequency-dependent regulation is actually through CSD, the time period of $[Ca^{2+}]_i$ reach-

ing the threshold level for the activation of a downstream event (20). In all previous studies mentioned above, regular $[Ca^{2+}]_i$ oscillations models were used. In those $[Ca^{2+}]_i$ oscillation models, frequency was always proportional to CSD because the amplitudes of spikes were constant. Obviously, this is not always the case for the biological $[Ca^{2+}]_i$ oscillations evoked by agonist stimulations, the parameters of which are not constant in general. In the current study focusing on irregular $[Ca^{2+}]_i$ oscillations, frequency is not always proportional to CSD as confirmed by regression analysis showing no significant correlation between frequency and CSD ($p > 0.05$ for regression analysis between frequency and CSD, supplemental Fig. S3, *a* and *b*). In support of this explanation, significant correlation between frequency and CSD as well as between frequency and nuclear translocation of NFκB and STAT3 is noted in the cells with the amplitude of each spike reaching the $[Ca^{2+}]_i$ threshold for NFκB or STAT3 activation, respectively (supplemental Fig. S4, *a* and *b*).

To characterize the mechanism underlying CSD-regulated NFκB activation by histamine-stimulated $[Ca^{2+}]_i$ oscillations in cells, we focused our effort on IκB-α phosphorylation, which liberates NFκB from cytosol into nucleus (30, 31). The IκB-α phosphorylation level was found to be regulated by irregular $[Ca^{2+}]_i$ oscillations also in a CSD-dependent way (Fig. $5a_i$). These experimental results coincide well with the prediction from the mathematical/computational modeling, indicating that IκB-α, not IKK, most sensitively determines the level of NFκB activity (32). Furthermore, the IL-8 mRNA expression, a downstream event of NFκB activation well established to be regulated by $[Ca^{2+}]_i$ oscillation frequency (17, 19, 20), is also obviously regulated in a CSD-dependent manner (Fig. $5b_i$). A similar mechanism and significance of CSD-dependent regulation of STAT3 activation were also revealed for JAK2 phosphorylation and VEGF expression (Fig. 5, a_{ii} and b_{ii}).

Variability of cell signaling in a cell and between cells is general (16, 33, 34) and insurmountable to our quantitative understanding the actual link between cellular signaling kinetics and its downstream events (29). Irregularity or kinetics of irregular $[Ca^{2+}]_i$ oscillations are regulated and or integrated by a variety of intracellular and extracellular conditions (12, 13, 16, 33, 34). The dynamic regulation of an agonist-stimulated transcription and gene expression by a manner combining $[Ca^{2+}]_i$ oscillation amplitude and cumulative spike duration is of general importance because $[Ca^{2+}]_i$ spike amplitude and cumulative spike duration can be separately and jointly modulated by many biological circumstances before they integrate as the final controller of transcription and gene expression.

REFERENCES

1. Berridge, M. J. (1990) Calcium oscillations. *J. Biol. Chem.* **265,** 9583–9586
2. Thomas, A. P. (1996) Spatial and temporal aspects of cellular calcium signalling. *FASEB J.* **10,** 1505–1517
3. Parekh, A. B. (2011) Decoding cytosolic Ca^{2+} oscillations. *Trends Biochem. Sci.* **36,** 78–87
4. Ridgway, E. B., and Durham, A. C. (1976) Oscillations of calcium ion concentrations in *Physarum polycephalum*. *J. Cell Biol.* **69,** 223–226
5. Woods, N. M., Cuthbertson, K. S., and Cobbold, P. H. (1986) Repetitive transient rises in cytoplasmic free calcium in hormone-stimulated hepatocytes. *Nature* **319,** 600–602
6. Marks, P. W., and Maxfield, F. R. (1990) Transient increases in cytosolic free calcium appear to be required for the migration of adherent human neutrophils. *J. Cell Biol.* **110,** 43–52
7. van den Pol, A. N., Finkbeiner, S. M., and Cornell-Bell, A. H. (1992) Calcium excitability and oscillations in suprachiasmatic nucleus neurons and glia *in vitro*. *J. Neurosci.* **12,** 2648–2664
8. Diliberto, P. A., Krishna, S., Kwon, S., and Herman, B. (1994) Isoform-specific induction of nuclear free calcium oscillations by platelet-derived growth factor. *J. Biol. Chem.* **269,** 26349–26357
9. Narenjkar, J., Marsh, S. J., and Assem, E. S. (1999) The characterization and quantification of antigen-induced Ca^{2+} oscillations in a rat basophilic leukaemia cell line (RBL-2H3). *Cell Calcium* **26,** 261–269
10. Heemskerk, J. W., Willems, G. M., Rook, M. B., and Sage, S. O. (2001) Ragged spiking of free calcium in ADP-stimulated human platelets: regulation of puff-like calcium signals *in vitro* and *ex vivo*. *J. Physiol.* **535,** 625–635
11. Zhang, M., Goforth, P., Bertram, R., Sherman, A., and Satin, L. (2003) The Ca^{2+} dynamics of isolated mouse beta-cells and islets: implications for mathematical models. *Biophys. J.* **84,** 2852–2870
12. Mohri, T., and Yoshida, S. (2005) Estrogen and bisphenol A disrupt spontaneous $[Ca^{2+}]_i$ oscillations in mouse oocytes. *Biochem. Biophys. Res. Commun.* **326,** 166–173
13. Hernández-SanMiguel, E., Vay, L., Santo-Domingo, J., Lobatón, C. D., Moreno, A., Montero, M., and Alvarez, J. (2006) The mitochondrial Na^+/Ca^{2+} exchanger plays a key role in the control of cytosolic Ca^{2+} oscillations. *Cell Calcium* **40,** 53–61
14. Martin-Cano, F. E., Gomez-Pinilla, P. J., Pozo, M. J., and Camello, P. J. (2009) Spontaneous calcium oscillations in urinary bladder smooth muscle cells. *J. Physiol. Pharmacol.* **60,** 93–99
15. Brasen, J. C., Olsen, L. F., and Hallett, M. B. (2011) Extracellular ATP induces spikes in cytosolic free Ca^{2+} but not in NADPH oxidase activity in neutrophils. *Biochim. Biophys. Acta* **1813,** 1446–1452
16. Thurley, K., and Falcke, M. (2011) Derivation of Ca^{2+} signals from puff properties reveals that pathway function is robust against cell variability but sensitive for control. *Proc. Natl. Acad. Sci. U.S.A.* **108,** 427–432
17. Dolmetsch, R. E., Xu, K., and Lewis, R. S. (1998) Calcium oscillations increase the efficiency and specificity of gene expression. *Nature* **392,** 933–936
18. Tomida, T., Hirose, K., Takizawa, A., Shibasaki, F., and Iino, M. (2003) NFAT functions as a working memory of Ca^{2+} signals in decoding Ca^{2+} oscillation. *EMBO J.* **22,** 3825–3832
19. Zhu, L., Luo, Y., Chen, T., Chen, F., Wang, T., Hu, Q. (2008) Ca^{2+} oscillation frequency regulates agonist-stimulated gene expression in vascular endothelial cells. *J. Cell Sci.* **121,** 2511–2518
20. Zhu, L., Song, S., Pi, Y., Yu, Y., She, W., Ye, H., Su, Y., and Hu, Q. (2011) Cumulated Ca^{2+} spike duration underlies Ca^{2+} oscillation frequency-regulated NFκB transcriptional activity. *J. Cell Sci.* **124,** 2591–2601
21. Turner, D. A., Paszek, P., Woodcock, D. J., Nelson, D. E., Horton, C. A., Wang, Y., Spiller, D. G., Rand, D. A., White, M. R., and Harper, C. V. (2010) Stochastic dynamics of NF-κB responses in single living cells. *J. Cell Sci.* **123,** 2834–2843
22. Berkova, Z., Morris, A. P., and Estes, M. K. (2003) Cytoplasmic calcium measurement in rotavirus enterotoxin-enhanced green fluorescent protein (NSP4-EGFP) expressing cells loaded with Fura-2. *Cell Calcium* **34,** 55–68
23. Wu, Y., and Clusin, W. T. (1997) Calcium transient alternans in blood-perfused ischemic hearts: observations with fluorescent indicator Fura Red. *Am. J. Physiol.* **273,** H2161–2169
24. Voronina, S., Sukhomlin, T., Johnson, P. R., Erdemli, G., Petersen, O. H., and Tepikin, A. (2002) Correlation of NADH and Ca^{2+} signals in mouse pancreatic acinar cells. *J. Physiol.* **539,** 41–52
25. Takahashi, A., Camacho, P., Lechleiter, J. D., and Herman, B. (1999) Measurement of intracellular calcium. *Physiol. Rev.* **79,** 1089–1125
26. Jin, S., Lu, D., Ye, S., Ye, H., Zhu, L., Feng, Z., Liu, S., Wang, D., and Hu, Q. (2005) A simplified probe preparation for ELISA-based NF-κB activity assay. *J. Biochem. Biophys. Methods* **65,** 20–29
27. Zhang, J., Zhou, J., Cai, L., Lu, Y., Wang, T., Zhu, L., and Hu, Q. (2012) Extracellular calcium-sensing receptor is critical in hypoxic pulmonary vasoconstriction. *Antioxid. Redox Signal.* **17,** 471–484
28. Dupont, G., and Combettes, L. (2009) What can we learn from the irreg-

ularity of Ca^{2+} oscillations? *Chaos* **19,** 037112
29. Dupont, G., Combettes, L., Bird, G. S., and Putney, J. W. (2011) Calcium oscillations. *Cold Spring Harbor Perspectives Biol.* **3,** 004226
30. Grilli, M., Pizzi, M., Memo, M., and Spano, P. (1996) Neuroprotection by aspirin and sodium salicylate through blockade of NF-κB activation. *Science* **274,** 1383–1385
31. DiDonato, J. A., Hayakawa, M., Rothwarf, D. M., Zandi, E., and Karin, M. (1997) A cytokine-responsive IκB kinase that activates the transcription factor NF-κB. *Nature* **388,** 548–554
32. Fisher, W. G., Yang, P. C., Medikonduri, R. K., and Jafri, M. S. (2006) NFAT and NFκB activation in T lymphocytes: a model of differential activation of gene expression. *Ann. Biomed. Eng.* **34,** 1712–1728
33. Skupin, A., and Falcke, M. (2007) Statistical properties and information content of calcium oscillations. *Genome Inform.* **18,** 44–53
34. Skupin, A., Kettenmann, H., Winkler, U., Wartenberg, M., Sauer, H., Tovey, S. C., Taylor, C. W., and Falcke, M. (2008) How does intracellular Ca^{2+} oscillate: by chance or by the clock? *Biophys. J.* **94,** 2404–2411